Qubit decoherence and non-Markovian dynamics at low temperatures via an effective spin-boson model

K. Shiokawa* and B. L. Hu†
Department of Physics, University of Maryland, College Park, Maryland 20742, USA
(Received 7 July 2004; published 9 December 2004)

Quantum Brownian oscillator model (QBM), in the Fock-space representation, can be viewed as a multilevel spin-boson model. At sufficiently low temperature, the oscillator degrees of freedom are dynamically reduced to the lowest two levels and the system behaves effectively as a two-level (E2L) spin-boson model (SBM) in this limit. We discuss the physical mechanism of level reduction and analyze the behavior of E2L-SBM from the QBM solutions. The availability of close solutions for the QBM enables us to study the non-Markovian features of decoherence and leakage in a SBM in the nonperturbative regime (e.g., without invoking the Born approximation) in better details than before. Our result captures very well the characteristic non-Markovian short time low temperature behavior common in many models.

DOI: 10.1103/PhysRevA.70.062106 PACS number(s): 03.65.Yz, 03.65.Ta, 03.67.Lx

I. INTRODUCTION

Recent development in quantum information processing and quantum computation has attracted much attention to the study of discrete quantum systems with finite degrees of freedom. The most commonly used model is an array of interacting two-level systems (2LS) each of which representing a qubit. As the system almost always interacts with its environment, quantum decoherence in the system usually is the most serious obstacle to the actual implementation of quantum information processors [1–3]. For this reason a detailed understanding of quantum decoherence in open systems is crucial. There are a handful of models useful for such studies, the quantum Brownian motion(QBM) [4–7] is one, the spin-boson model [4,8] is another: the system in the former case is a harmonic oscillator and in the latter case a 2LS, both interacting with an environment of a harmonic oscillator bath (HOB).

Most qubit models presently employed are the results of picking out the levels most relevant to the description of the qubit from a multilevel structure. In atom optics, internal electronic excitations are often approximated by a 2LS consisting of the ground state and the excited state. A similar model is used for the study of low temperature tunneling process where the two levels degrees of freedom represent the quasi ground states in a double well potential. The simplification to two-levels allows for detailed analytical or numerical treatment, but this remains an approximation applicable only when the effects of higher levels are negligible, e.g., at low enough temperature when higher levels are not well-populated. However, in the presence of gate operation, the existence of higher levels causes a leakage of the 2LS due to transitions to these other levels. Some extra perturbation may be necessary to select or restrict multi-level structure the particular levels of interest [9]. In order to make a quantitative estimation of decoherence with a leakage effect, it is more desirable to study open system models which maintain the multilevel structure.

In the present paper, we study certain aspects of realistic qubits residing in the multilevel system, taking advantage of our fairly good understanding from the detailed studies of QBM over the last few decades. In particular, we focus on harmonic QBM, which can be viewed as an ∞-level spin-boson model. Commonly used two-level spin-boson model can be obtained by restricting the harmonic oscillator Fock space to the lowest two levels. This correspondence allows for a detailed analysis of the spin-boson model from the known results of QBM. In particular, we will focus on the *non-Markovian* aspects of decoherence. Non-Markovian dynamics, often neglected in the literature (models are mainly based on a Markov approximation) for technical simplicity, is actually of crucial importance for the realistic implementations of quantum information processing. The "effective" model we consider here invokes a two level simplification from a multilevel structure. How realistic this is certainly depends on the way the qubits are defined and realized in the multilevel structure usually encountered in actual experimental conditions. Nevertheless, our model is able to capture the characteristic short time behavior in many physical examples.

Beyond the commonly assumed Ohmic spectrum for the bath, generic non-Ohmic environments can be studied with this model. Contrary to the Ohmic case, the sub-Ohmic environment (including $1/f^{\alpha}$ type) causes nontrivial long time behavior such as anomalous diffusion or localization [8] owing to the long range temporal bath correlation. In the present paper, we will mainly focus on the opposite case of super-Ohmic environments [4,8,27]. Owing to the ultrashort time bath correlations, nontrivial short-time system dynamics enters, which is particularly difficult to describe by means of other models or approximations. The decoherece time scale in the super-Ohmic environment can be much shorter than the one in the Ohmic case and thus is hard to remove by external pulses. Thus super-Ohmic environment can be a major obstacle for the realization of quantum computation and information processing.

*Email address: kshiok@physics.umd.edu
†Email address: hub@physics.umd.edu

We emphasize that to maximally preserve the coherence of an open system, self-consistency is required, and because of the back-action from the environment, non-Markovian processs is often the norm rather than the exception. We will argue that, for a generic class of environment, Markovian approximations are not strictly valid. To facilitate comparison with results in related papers we will compare our methods with other commonly used approximations to the spin-boson model, such as the Born approximation and the Born-Markov rotating-wave approximation [10] for two-level and multilevel systems.

The outline of this paper is as follows: In Sec. II we specify the model and cast it in the influence functional formalism in the presence of an external field. In Sec. III we outline our idea of an effective 2LS using the QBM approach. Then we make correspondence between the phase space representation discussed in Sec. II with the Fock space representation. We compare our approach with other methods based on Born-Markov and rotating-wave-approx imation. Our results are presented in Sec. IV A. In Sec. IV B we discuss the limitations and potential extensions of this approach.

II. QBM IN THE PRESENCE OF AN EXTERNAL FIELD

A. The model

Our model consists of a Brownian particle interacting with a thermal bath in the presence of an external field. We follow the notion developed in [6,12]. (We use the units in which $k_B=\hbar=1$.) The Hamiltonian for this model can be written as

$$H = H_S + H_B + H_I + H_F, \tag{1}$$

where the dynamics of the system S (with coordinate x and momentum p) is described by the Hamiltonian

$$H_S = \frac{p^2}{2M} + V_0(x), \tag{2}$$

and the (bare) potential $V_0(x)$ is related to the physical potential by a counter term ΔV i.e., $V_0(x)=V(x)+\Delta V$ (see below). The bath is assumed to be composed of N harmonic oscillators with natural frequencies ω_n and masses m_n with Hamiltonian

$$H_B = \sum_{n=1}^{N}\left(\frac{p_n^2}{2m_n} + \frac{m_n\omega_n^2 q_n^2}{2}\right), \tag{3}$$

where $(q_1,\ldots,q_N,p_1,\ldots,p_N)$ are the coordinates and their conjugate momenta. The interaction between the system S and the bath B is assumed to be bilinear,

$$H_I = x\sum_{n=1}^{N} c_n q_n, \tag{4}$$

where c_n is the coupling constant between the Brownian oscillator and the nth bath oscillator with coordinate q_n. The coupling constants are related to the spectral density $J_B(\omega)$ of the bath by

$$J_B(\omega) \equiv \pi\sum_n \frac{c_n^2}{2m_n\omega_n}\delta(\omega-\omega_n). \tag{5}$$

We assume the spectral density has the form

$$J_B(\omega) = 2M\gamma\omega^\nu e^{-\omega/\Lambda}, \tag{6}$$

where $\nu=1$ is Ohmic, $\nu<1$ is sub-Ohmic, and $\nu>1$ is super-Ohmic. We will discuss the Ohmic and super-Ohmic ($\nu=3$) cases in detail.

The counterterm ΔV depends on c_n, m_n, ω_n, p and x and is given by

$$\Delta V = \begin{cases} 2M\gamma\Lambda x^2/\pi & (\nu=1), \\ 2M\gamma\Lambda p^2/M^2\pi + 2M\gamma\Lambda^3 x^2/\pi & (\nu=3). \end{cases} \tag{7}$$

This term is introduced to cancel the shift in the mass and frequency of the Brownian oscillator due to its interaction with the bath which will become divergent when the frequency cutoff $\Lambda\to\infty$. As is customary, we consider the renormalized quantities after including a counter term as the physical observables with specified values.

For a linear QBM, the potential is

$$V(x) = \frac{M\Omega^2 x^2}{2}, \tag{8}$$

where Ω is the natural frequency of the system oscillator. Finally, the Hamiltonian for the external field $E(t)$ is assumed to be

$$H_F = -xE(t). \tag{9}$$

B. The influence functional

We begin by making the connection with prior treatment of QBM based on the influence functional [13] with a phase space representation for the Wigner function [14]. First we consider the case without an environment. We define the transition amplitude between the initial state $|x_0 q_0\rangle$ at $t=0$ and the final state $|x\ q\rangle$ at time t to be

$$K(x,q;t|x_0,q_0;0) \equiv \langle x\ q|e^{-iHt}|x_0 q_0\rangle. \tag{10}$$

The Liouville equation for the density matrix is

$$i\frac{\partial}{\partial t}\rho(t) = [H,\rho(t)], \tag{11}$$

where [,] is the commutator. In the coordinate representation, the density matrix becomes

$$\rho(x,x',q,q',t) \equiv \langle x\ q|\rho(t)|x'q'\rangle, \tag{12}$$

with the collective notation for bath variables $q\equiv\{q_n\}$. The time evolution of the density matrix is given by

$$\rho(x,x',q,q',t) = \int dx_0 dx_0' dq_0 dq_0' K(x,q;t|x_0,q_0;0) \times\rho(x_0,x_0',q_0,q_0',0)K^*(x',q';t|x_0',q_0';0). \tag{13}$$

For the problem under study, we assume that the characteristic time scale for the bath is much shorter than the sys-

tem. Under this condition, we may integrate out the bath harmonic oscillator variables to obtain an equation for the reduced density matrix $\rho_r(x,x') \equiv \int dq \rho(x,x',q,q,t)$. For a factorized initial condition between the system and the bath, which is assumed to be initially in thermal equilibrium,

$$\rho(x_0,x_0',q_0,q_0',0) = \rho_S(x_0,x_0',0) \otimes \rho_B(q_0,q_0',0), \tag{14}$$

we can express the time evolution for the reduced density matrix in an integral form,

$$\rho_r(x,x',t) = \int dx_0 dx_0' J_r(x,x';t|x_0,x_0';0)\rho_S(x_0,x_0',0), \tag{15}$$

where its time evolution operator is given by

$$J_r(x,x';t|x_0,x_0';0) = \int dq dq_0 dq_0' K(x,q;t|x_0,q_0;0) \times \rho_B(q_0,q_0',0) K^*(x',q;t|x_0',q_0';0). \tag{16}$$

The total action of the system $\mathcal{S}[x,x']$ enters as

$$J_r(x,x';t|x_0,x_0';0) \equiv \int_{(x_0x_0')}^{(xx')} \mathcal{D}x\mathcal{D}x' e^{i\mathcal{S}[x,x']} \tag{17}$$

and consists of several contributions:

$$\mathcal{S}[x,x'] = \mathcal{S}_S[x,x'] + \Delta\mathcal{S}_C[x,x'] + \mathcal{S}_F[x,x'] + \mathcal{S}_{IF}[x,x']. \tag{18}$$

The sum of the actions for the system $\mathcal{S}_S$ plus its counteraction $\Delta\mathcal{S}_S$ is given by

$$(\mathcal{S}_S + \Delta\mathcal{S}_S)[R,r] = \int_0^t ds\{M_0\dot{R}(s)\dot{r}(s) - M_0\Omega_0^2 R(s)r(s)\}, \tag{19}$$

where $R \equiv (x+x')/2, r \equiv x-x'$. For notational convenience, we have assumed the bare mass M_0 and bare frequency Ω_0 take on the values $M_0 = M$ and $M_0\Omega_0^2 = M\Omega^2 + 4M\gamma\Lambda/\pi$ for $\nu=1$ while $M_0 = M + 4M\gamma\Lambda/\pi$ and $M_0\Omega_0^2 = M\Omega^2 + 4M\gamma\Lambda^3/(3\pi)$ for $\nu=3$. The action for the external field is

$$\mathcal{S}_F[R,r] = \int_0^t ds\, r(s)E(s). \tag{20}$$

The influence action $\mathcal{S}_{IF}[x,x']$ accounts for the effect of the bath on S and is given by

$$\mathcal{S}_{IF}[R,r] = i\int_0^t ds \int_0^s ds' r(s)\mu(s-s')r(s') - 2\int_0^t ds \int_0^s ds' r(s)\nu(s-s')R(s'), \tag{21}$$

where

$$\nu(t) = \frac{1}{\pi}\int_0^\infty d\omega\, J_B(\omega)\coth\frac{\beta\omega}{2}\cos\omega t, \tag{22}$$

$$\mu(t) = -\frac{1}{\pi}\int_0^\infty d\omega\, J_B(\omega)\sin\omega t \tag{23}$$

are the noise and dissipation kernels, respectively.

From Eqs. (21) the Euler-Lagrange equations for R and r are

$$M_0\ddot{R}_c(t) + M_0\Omega_0^2 R_c(t) + 2\int_0^t ds\ \mu(t-s)R_c(s) = E(t), \tag{24}$$

$$M_0\ddot{r}_c(s) + M_0\Omega_0^2 r_c(s) - 2\int_s^t ds'\mu(s-s')r_c(s') = 0. \tag{25}$$

The nonlocal kernel μ contains the information of the past history of the bath in the presence of the system variables. Thus by solving these equations, self-consistency of the system-bath interaction is taken into account. Nonlocal kernels imply that these equations normally contain time derivatives higher than two. In earlier studies of QBM, higher order terms were neglected [11]. Hence the damping effect was not treated properly. Inclusion of the higher order terms leads to unphysical runaway solutions. In [12], the order reduction procedure similarly to the radiation damping problem is used to eliminate unphysical solutions reducing them into second order differential equations with well-defined initial value problems. After the order reduction procedure, the solutions can be specified uniquely by imposing the initial and final conditions: R_0 and R_t (r_0 and r_t).

If we let the two independent solutions of the homogeneous part of Eq. (24) and Eq. (25) be $u_i(s)$ and $v_i(s), i=1, 2$, with boundary conditions $u_1(0)=1, u_1(t)=0, u_2(0)=0, u_2(t)=1$ and $v_1(0)=1, v_1(t)=0, v_2(0)=0, v_2(t)=1$, respectively, the solutions of these uncoupled equations can be written as

$$R_c(s) = R_0u_1(s) + R_tu_2(s) + e(s),$$

$$r_c(s) = r_0v_1(s) + r_tv_2(s), \tag{26}$$

where $e(t) = \int_0^t ds g_+(t-s)E(s)/M$. The solutions v_1 and v_2 satisfy the homogeneous part of the backward time equation (25) and are related to u_1 and u_2 by $v_1(s) = u_2(t-s)$ and $v_2(s) = u_1(t-s)$. The functions $g_+(s)$ and $g_-(s)$ also satisfies the homogeneous part of Eq. (24) and Eq. (25) with boundary conditions $g_\pm(0) = 0, \dot{g}_\pm(0) = 1$, respectively. The solutions for $g_\pm$ for Ohmic and super-Ohmic cases are given in Appendix A of [12]. From these solutions $u_{1,2}$ and $v_{1,2}$ can be determined.

Since the potentials in our model are harmonic, an exact evaluation of the path integral can be carried out. It is dominated by the classical solution given in Eq. (26). From these classical solutions, we write the action $\mathcal{S}[x,x']$ as

$$\mathcal{S}[R_c,r_c] = [M\dot{u}_1(t)R_0 + M\dot{u}_2(t)R_t]r_t - [M\dot{u}_1(0)R_0 + M\dot{u}_2(0)R_t]r_0 + i\{a_{11}(t)r_0^2 + [a_{12}(t) + a_{21}(t)]r_0r_t + a_{22}(t)r_t^2\} + e_1(t)r_0 + e_2(t)r_t. \tag{27}$$

Here $\mathbf{(}e_1(t),e_2(t)\mathbf{)}=e^T=\int_0^t ds\mathbf{(}v_1(s),v_2(s)\mathbf{)}e(s)$ and

$$a_{kl}(t)=\frac{1}{2}\int_0^t ds\int_0^t ds' v_k(s)\mu(s-s')v_l(s'), \tag{28}$$

for $(k,l=1,2)$ contains the effects of induced fluctuations from the bath on the system dynamics.

Using the results above, J_r in Eq. (17) can be written in the compact form,

$$J_r(R_t,r_t;t|R_0,r_0;0)=N(t)e^{i\mathcal{L}}, \tag{29}$$

where $\mathcal{L}=\boldsymbol{R}^T\boldsymbol{u}\boldsymbol{r}+i\boldsymbol{r}^T\boldsymbol{a}\boldsymbol{r}+\boldsymbol{e}^T\boldsymbol{r}$, $(\boldsymbol{a})_{ij}=a_{ij}$, $\boldsymbol{R}^T=(R_0,R_t)$, and $\boldsymbol{r}^T=(r_0,r_t)$,

$$\boldsymbol{u}=\begin{pmatrix}u_{11} & u_{12}\\ u_{21} & u_{22}\end{pmatrix}\equiv M\begin{pmatrix}-\dot{u}_1(0) & \dot{u}_1(t)\\ -\dot{u}_2(0) & \dot{u}_2(t)\end{pmatrix}. \tag{30}$$

C. QBM in the phase space representation

The Wigner function is related to the density matrix by

$$W_r(R,P,t)=\frac{1}{2\pi}\int dr\, e^{-iPr}\rho_r(R+r/2,R-r/2,t). \tag{31}$$

The Wigner distribution function obeys the evolution equation

$$W_r(R_t,P_t,t)=\int dR_0dP_0K(R_t,P_t;t|R_0,P_0;0)W_r(R_0,P_0,0), \tag{32}$$

where $K(R,P;t|R_0,P_0;0)$ is defined by

$$K(R,P;t|R_0,P_0;0)=\frac{1}{2\pi}\int dr\, dr_0e^{-i(Pr-P_0r_0)}J_r(R,r;t|R_0,r_0;0). \tag{33}$$

The propagator K for the Wigner function is given by

$$K(R,P;t|R_0,P_0;0)=\frac{N(t)}{2\pi}\int dr\, dr_0e^{i(-P_r+P_0r_0+\mathcal{L})}$$
$$=N_W(t)\exp[-\delta\vec{X}^T\Sigma^{-1}\delta\vec{X}],$$

where $N_W(t)=N(t)/2\sqrt{|\boldsymbol{a}|}$ and $|\boldsymbol{a}|$ is the determinant of $\boldsymbol{a}$. The vector $\delta\vec{X}=\vec{X}-\langle\vec{X}\rangle$, with

$$\vec{X}=\begin{pmatrix}R\\ P-e_2\end{pmatrix}, \tag{34}$$

and

$$\langle\vec{X}\rangle=\begin{pmatrix}\langle R\rangle\\ \langle P\rangle\end{pmatrix}=\begin{pmatrix}C_{11} & C_{21}\\ C_{12} & C_{22}\end{pmatrix}\begin{pmatrix}R_0\\ P_0+e_1\end{pmatrix}$$
$$=\frac{-1}{u_{21}}\begin{pmatrix}u_{11} & 1\\ |\boldsymbol{u}| & u_{22}\end{pmatrix}\begin{pmatrix}R_0\\ P_0+e_1\end{pmatrix}. \tag{35}$$

Here Σ is a matrix characterizing the induced fluctuations from the environment:

$$\Sigma=\frac{2}{u_{21}^2}\begin{pmatrix}a_{11} & a_{12}u_{21}-a_{11}u_{22}\\ a_{12}u_{21}-a_{11}u_{22} & a_{11}u_{22}^2-2a_{12}u_{21}u_{22}+a_{22}u_{21}^2\end{pmatrix}. \tag{36}$$

At long times, fluctuations of the system are governed by these terms as $\Sigma_{11}\to\langle(\Delta R)^2\rangle$, $\Sigma_{22}\to\langle(\Delta P)^2\rangle$, and $\Sigma_{12}=\Sigma_{21}\to 0$.

It is seen that this solution for the density matrix obeys non-Markovian dynamics in that the solution at a given time depends on its past history. Owing to the time dependent nature of their coefficients, despite its simple appearance, these equations are not easy to solve without approximations. The commonly used Markovian approximations can miss the essential features in the description of quantum/classical correspondence: it tends to underestimate the loss of quantum coherence because the rapid initial increase of diffusion coefficients is crucial for decoherence at low temperature for strong coupling. It is simply not a valid approximation for a harmonic oscillator model with a generic spectral density.

III. EFFECTIVE SPIN-BOSON MODEL FROM QBM

A. Dynamical level reduction

We first illustrate our scheme of dynamical level reduction based on the harmonic QBM, which can be viewed as an infinite-level system in a bosonic environment

$$H_S^{(\infty)}+H_I^{(\infty)}=\Omega a^\dagger a+\sqrt{2\Omega}(a+a^\dagger)\sum_{n=1}^{N_B}c_nq_n. \tag{37}$$

This can be viewed as a limit of the finite N-level system:

$$H_S^{(N)}+H_I^{(N)}=\Omega S_N^+S_N^-+(S_N^-+S_N^+)\sum_{n=1}^{N_B}\tilde{c}_nq_n \tag{38}$$

when $N\to\infty$. Here we have absorbed $\sqrt{2\Omega}$ by defining $\tilde{c}_n=\sqrt{2\Omega}c_n$.

At finite temperature T, only those modes up to $N\sim k_BT/\hbar\Omega$ are occupied. Thus at low temperature $T\sim\hbar\Omega$, the effective number of levels of harmonic QBM is significantly reduced. In particular, at $k_BT<\hbar\Omega$, we expect that the system is effectively reduced to two levels:

$$H_S^{(2)}+H_I^{(2)}=\Omega S_2^+S_2^-+(S_2^-+S_2^+)\sum_{n=1}^{N_B}\tilde{c}_nq_n. \tag{39}$$

The formal correpondence is achieved by replacing the harmonic oscillator annihilation/creation operator $a,a^\dagger$ by the two-level pseudospin annihilation/creation (Pauli) operator S_2^-,S_2^+. The spin-boson model can be obtained by rewriting the Pauli operators as

$$H_S^{(2)}+H_I^{(2)}=\Omega\left(S_2^z+\frac{1}{2}\right)+S_2^x\sum_{n=1}^{N_B}\tilde{c}_nq_n. \tag{40}$$

B. Fock states from phase space representation

The correspondence between the Fock state representation for the pseudospin qubits and the phase space representation

is given as follows. First we write the density matrix in terms of the phase space variable as

$$\hat{\rho}(t) = \int \frac{d^2z}{\pi} \chi_Q(z,\bar{z},t) e^{-iz\bar{a}^\dagger} e^{-iza}, \tag{41}$$

where

$$\chi_Q(z,\bar{z},t) = \mathrm{Tr}[\hat{\rho}(t) e^{iza} e^{iz\bar{a}^\dagger}] \tag{42}$$

is a characteristic function for the Q (or Hushimi) representation [15,16]. In a Fock space representation,

$$\rho_{kl}(t) = \int \frac{d^2z}{\pi} \chi_Q(z,\bar{z},t) \langle k| e^{-iz\bar{a}^\dagger} e^{-iza} |l\rangle, \tag{43}$$

$\chi_Q(z,\bar{z})$ is related to the characteristic function for the Wigner representation $\chi_W(z,\bar{z})$ by

$$\chi_Q(z,\bar{z},t) = e^{-|z|^2/2} \chi_W(z,\bar{z},t). \tag{44}$$

These characteristic functions are Fourier components of the phase space distribution functions, namely

$$\chi_Q(z,\bar{z},t) = \int d^2\alpha Q(\alpha,\bar{\alpha}) e^{iz\bar{\alpha}} e^{iz\alpha}, \tag{45}$$

$$\chi_W(z,\bar{z},t) = \int d^2\alpha W(\alpha,\bar{\alpha}) e^{iz\bar{\alpha}} e^{iz\alpha}. \tag{46}$$

The characteristic function $\chi_Q(z,\bar{z},t)$ for the harmonic QBM evolved from the initial ground state has the following Gaussian form:

$$\chi_Q(z,\bar{z},t) = \exp\left[-\frac{\langle a^2(t)\rangle}{2} z^2 - \frac{\langle a^{\dagger 2}(t)\rangle}{2} \bar{z}^2 - \langle a(t)a^\dagger(t)\rangle |z|^2 + i\alpha_f(t) z + i\bar{\alpha}_f(t)\bar{z} \right]. \tag{47}$$

The time dependent coefficients are antinormal ordered operator averages of second moments given by $\langle a^2\rangle = c + \sigma, \langle aa^\dagger\rangle = C + \Sigma + 1/4$, and α_f, which have their origins in the classical trajectory $\boldsymbol{C}$ of a damped harmonic oscillator in Eq. (35), the induced fluctuations Σ from the bath in Eq. (36), and the external field E. The relations of these components are given as follows:

$$8c = C_{22}^2 - C_{11}^2 + \Omega^2 C_{12}^2 - \frac{C_{21}^2}{\Omega^2} + 2i(C_{11}C_{12} + C_{21}C_{22}),$$

$$8C = C_{11}^2 + \Omega^2 C_{12}^2 + \frac{C_{21}^2}{\Omega^2} + C_{22}^2,$$

$$4\sigma = \Omega\Sigma_{11} - \frac{\Sigma_{22}}{\Omega} + 2i\Sigma_{12},$$

$$4\Sigma = \Omega\Sigma_{11} + \frac{\Sigma_{22}}{\Omega}, \tag{48}$$

and

$$\alpha_f(t) = \frac{1}{\sqrt{2\Omega}} \int_0^t \left(\Omega + i\frac{d}{dt} \right) g_+(t-s) E(s), \tag{49}$$

where g_+ satisfies the homogeneous part of the equation of motion in Eq. (24).

From Eq. (43) we can directly evaluate the density matrix in the Fock representation at arbitrary quantum number. Note that Fock states are not Gaussian states in general. For instance, for an initial ground state, $\hat{\rho}(0) = |0\rangle\langle 0|$, in the absence of an external field, the ground state and the first excited state population can be written as

$$\rho_{00}(t) = \frac{1}{[\langle aa^\dagger\rangle^2 - \langle a^2\rangle\langle a^{\dagger 2}\rangle]^{1/2}} \tag{50}$$

and

$$\rho_{11}(t) = \frac{1}{[\langle aa^\dagger\rangle^2 - \langle a^2\rangle\langle a^{\dagger 2}\rangle]^{1/2}} - \frac{\langle aa^\dagger\rangle}{[\langle aa^\dagger\rangle^2 - \langle a^2\rangle\langle a^{\dagger 2}\rangle]^{3/2}}. \tag{51}$$

Let us introduce the Pauli spin representation for the two-level system:

$$\langle \sigma_x(t)\rangle = \rho_{01}(t) + \rho_{10}(t),$$

$$\langle \sigma_y(t)\rangle = i\rho_{10}(t) - i\rho_{01}(t),$$

$$\langle \sigma_z(t)\rangle = \rho_{11}(t) - \rho_{00}(t). \tag{52}$$

We can express them by the variables defined in Eqs. (47)–(49) for arbitrary two-level spin initial states as follows:

$$\langle \sigma_x(t)\rangle = \frac{-1}{[\langle aa^\dagger\rangle^2 - \langle a^2\rangle\langle a^{\dagger 2}\rangle]^{3/2}} \left\{ [\langle \sigma_x(0)\rangle C_{22} - \langle \sigma_y(0)\rangle \Omega C_{12}] \times [\mathrm{Re}\langle a^2\rangle - \langle aa^\dagger\rangle] + \left[\langle \sigma_x(0)\rangle \frac{C_{21}}{\Omega} - \langle \sigma_y(0)\rangle C_{11} \right] \mathrm{Im}\langle a^2\rangle \right\}, \tag{53}$$

$$\langle \sigma_y(t)\rangle = \frac{-1}{[\langle aa^\dagger\rangle^2 - \langle a^2\rangle\langle a^{\dagger 2}\rangle]^{3/2}} \left\{ \left[\langle \sigma_x(0)\rangle \frac{C_{21}}{\Omega} - \langle \sigma_y(0)\rangle C_{11} \right] \times [\mathrm{Re}\langle a^2\rangle + \langle aa^\dagger\rangle] - [\langle \sigma_x(0)\rangle C_{22} - \langle \sigma_y(0)\rangle \Omega C_{12}] \mathrm{Im}\langle a^2\rangle \right\}, \tag{54}$$

and

$$\langle \sigma_z(t)\rangle = -\frac{\langle aa^\dagger\rangle}{[\langle aa^\dagger\rangle^2 - \langle a^2\rangle\langle a^{\dagger 2}\rangle]^{3/2}} + \frac{4\rho_{11}(0)}{[\langle aa^\dagger\rangle^2 - \langle a^2\rangle\langle a^{\dagger 2}\rangle]^{3/2}} \left\{ \mathrm{Re}[\bar{c}\langle a^2\rangle] - C\langle aa^\dagger\rangle - C + 6\langle aa^\dagger\rangle \frac{\mathrm{Re}[\bar{c}\langle a^2\rangle] - C\langle aa^\dagger\rangle}{[\langle aa^\dagger\rangle^2 - \langle a^2\rangle\langle a^{\dagger 2}\rangle]^{3/2}} \right\}. \tag{55}$$

These identities relate expectation values in oscillator variables and effective spin variables. In particular, the close

relations between the time dependent nonequilibrium uncertainty principle and decoherence and dissipation in the low level excitations become manifest. The uncertainty principle generalized for mixed states in nonequilibrium implies that $\langle aa^{\dagger}\rangle^2-\langle a^2\rangle\langle a^{\dagger 2}\rangle \geqslant 1$, which gives $\rho_{00}(t)\leqslant 1$ in Eq. (50). Thus the positivity of the density matrix ρ_{00} is guaranteed by the uncertainty principle. Uncertainties of oscillator variables will manifest themselves in a temporal decay of number states and can be observed, for instance, in Rabi oscillations. Conversely, the crossover between the qubit decoherence from quantum fluctuation dominated regime to thermal fluctuation dominated regime [12,17] implies the similar quantum to classical crossover exists in the time-dependent uncertainties in the phase space [5].

The leakage at time t is given by $\mathcal{L}(t)=1-\min \mathrm{Tr}[\hat{P}\rho_r(t)]$, where $\hat{P}$ is the projection operator onto the computational subspace and the minimization is taken over initial conditions. In our case, $\hat{P}=\Sigma_{n=0,1}|n\rangle\langle n|$. The source of the leakage in our model is the transition to higher modes. The leakage is typically estimated by perturbative methods. However, the exact temporal evolution of this function is highly nontrivial as we will see below. Note that from the form of our *effective* Hamiltonian in Eq. (40), the notion of coherence and population between our model and some others in the literature (for example, in [8]) are interchanged. They are related to each other by a change of basis. We can obtain similar expressions in the presence of an external field. We will examine this case in Sec. IV A. In the Markovian limit, if the limit exists, two-level spin states become coupled nontrivially and obey optical-Bloch type equations [18].

C. Limitations of other approximations

1. Born approximation

Although exact master equations for open systems are integro-differential equations, they can also be written in a time-convolutionless form [29] (differential equation with time-dependent coefficients local in time). The master equations in this form are still difficult to deal with. Most approaches based on master equations invoke Born-approximation, which is not applicable for strong coupling and the bath with long range correlation. Under Born-approximation, one can obtain a tractable form, which can be solved numerically [20] or analytically in some cases [21]. The master equation under weak-coupling approximation may be suitable for describing the short time dynamics but tends to predict incorrect behavior for long times [4,8]. Our nonperturbative approach does not require Born approximation and thus is applicable to arbitrary time scales.

2. Born-Markov approximation

In this approximation, the bath correlation is neglected. This may be obtained as a limit of high temperature or adiabatic system evolution in the Ohmic bath. For a generic bath spectral density, however, there is no such limit. In a super-Ohmic bath, the bath correlation, when time-averaged for a long time, vanishes owing to the ultrashort time correlation time. In a sub-Ohmic bath, it diverges owing to the long correlation time. Only Ohmic spectrum gives the finite constant diffusion term.

3. Born-Markov rotating-wave-approximation

For weak coupling, the off-resonant counter-rotating terms in the interaction Hamiltonian are often ignored by invoking the rotating-wave-approximation (RWA). Although the use of RWA significantly simplifies the analysis, the dynamics under this approximation cannot capture the fast dynamics at time scales less than the natural time scale of the system. Furthermore, the spectrum of the Hamiltonian under RWA is found to be unbounded from below [19]. These features suggest that the range of validity of RWA is restricted to the leading order in the coupling constant only, where the counter-rotating terms do not contribute. After neglecting the counter-rotating terms from the two-level spin-boson Hamiltonian in Eq. (40), we obtain

$$H_S+H_{SB}=\Omega S_2^+S_2^-+(S_2^-+S_2^+)\sum_{n=1}^{N}c_nq_n \rightarrow H_S+H_{RWA}$$
$$=\Omega S_2^+S_2^-+\sum_{n=1}c_n(S_2^-b_n^{\dagger}+S_2^+b_n), \tag{56}$$

where $b_n=(\omega_nq_n+ip_n)/\sqrt{2\omega_n}$ are bath annihilation operators. In the presence of an external field, under the RWA, the reduced density matrix for the Hamiltonian obeys an optical Bloch equation. This case is commonly described in quantum optics text books.

4. Born-Markov-RWA in multilevel system (MLS)

For comparison, we make the same Born-Markov-RWA in our E2L-SBM. Since the naive high temperature limit of the master equation obtained from QBM violates positivity [28], we start from the master equation in the Lindblad form [10]. For a particle initially in the Fock state $\hat{\rho}(0)=|k\rangle\langle k|$, the Q distribution function at time t has the following form:

$$Q(\alpha,\overline{\alpha})=\frac{1}{\pi[1+n_B(1-e^{-\gamma t})]}\exp\left[-\frac{|\alpha|^2}{1+n_B(1-e^{-\gamma t})}\right]$$
$$\times\left[\frac{(n_B+1)(1-e^{-\gamma t})}{1+n_B(1-e^{-\gamma t})}\right]^k\sum_{l=0}^{k}\frac{1}{k!}\frac{k!}{l!\,(k-l)!}$$
$$\times\left[\frac{|\alpha|^2e^{-\gamma t}}{(n_B+1)(1-e^{-\gamma t})\{1+n_B(1-e^{-\gamma t})\}}\right]^l, \tag{57}$$

where $n_B\equiv 1/(e^{\beta\Omega}-1)$ is a Planck distribution factor. For $\hat{\rho}(0)=|1\rangle\langle 1|$, from Eqs. (43), (45), and (57),

$$\rho_{00}(t)=\frac{1}{[1+n_B(1-e^{-\gamma t})]^2}[1-e^{-\gamma t}+n_B(1-e^{-\gamma t})] \tag{58}$$

and

$$\rho_{11}(t)=\frac{1}{1+n_B(1-e^{-\gamma t})}\left\{1-\frac{1+e^{-\gamma t}}{1+n_B(1-e^{-\gamma t})}\right.$$
$$\left.+\frac{2e^{-\gamma t}}{[1+n_B(1-e^{-\gamma t})]^2}\right\}. \tag{59}$$

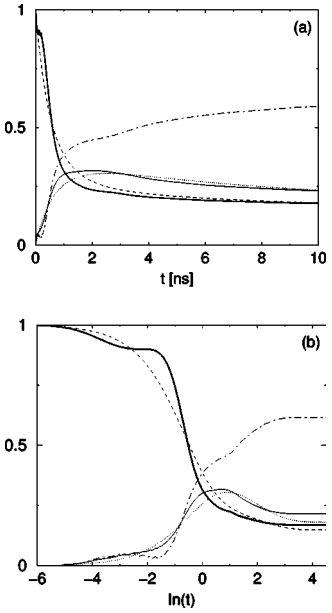

FIG. 1. (a) Plot of the time evolution of the population of the ground and the first excited state population, and the leakage (the dot-dashed curve) at $T=50$ mK with $\Omega=1$ GHz, $\gamma=0.1$ GHz, and $\Lambda=100$ GHz. The thick solid (dashed) curve is the exact (Markovian) result for excited states while the thin solid (dashed) curve is the exact (Markovian) result for ground states. Panel (b) is in the logarithmic time scale.

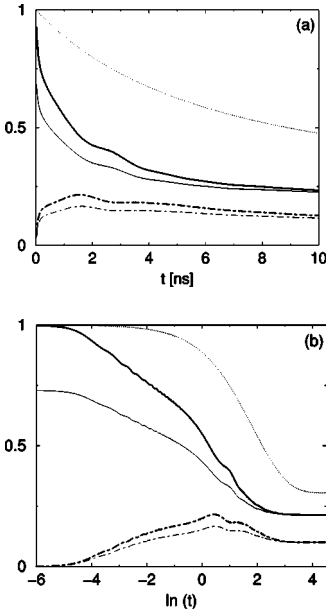

FIG. 2. The ground and the first excited state population, and the leakage (the dot-dashed curve) at $T=10$ mK. $\Omega=1$ GHz, $\gamma=0.1$ GHz, and $\Lambda=100$ GHz. The thick (thin) curve is for the excited state with the pure (mixed) state initial condition. Panel (b) is in the logarithmic time scale.

IV. RESULTS AND DISCUSSIONS

A. Results

In Fig. 1, the populations and the leakage at $T=50$ mK, $\Omega=1$ GHz, $\gamma=0.1$ GHz, and $\Lambda=100$ GHz are shown. The initial state is assumed to be the first excited state. At this temperature, the exact and the Markovian results agree at an intermediate time scale (around $t=10$ ns) but disagree at initial times. The slow oscillations in Fig. 1(b) of the exact curve are from effects due to counter-rotating terms. The large leakage indicates that at this temperature, $k_BT>\hbar\Omega$, 2LS description is not a good picture. In Fig. 2, $T=10$ mK case is shown. There is a drastic difference in the entire time range shown in the figure. The exact result follows the quick decay at early times up to $t\sim10-50$ ps. Late time decay rate asymptotically approaches the value given by the Markov approximation. The leakage is relatively large initially but negligibly small at late times. This indicates that only the lowest two levels are essentially populated except for the initial times, $t<5$ ns. The initial rapid decay of population is the result of large initial leakage due to the transition to noncomputational subspace. The large initial impact of the bath also appears in the diffusion constants in the generalized master equation at low temperature. (Note that at low temperature, there is also an anomalous diffusion constant [6].) The total decay slows down as the leakage is suppressed at an intermediate time scale. The qualitative features are unchanged for the more realistic mixed state initial condition (starting from the local equilibrium with the lowest two population reversed) except for the initial value, which is shifted to below unity. In Fig. 3(a), the decay rate of the excited state population at $T=0$ is plotted. The large initial growth is due to the rapid decoherence which sets in around the bath characteristic time scale. The rate reaches the value given by the Markovian approximation asymptotically. The Born-Markov RWA prediction from 2LS and multilevel system (MLS) (dashed line) coincide since there is no excitation from the ground state at $T=0$ under RWA. In Fig. 3(b) the same quantity at $T=20$ mK is shown. The decay rate under

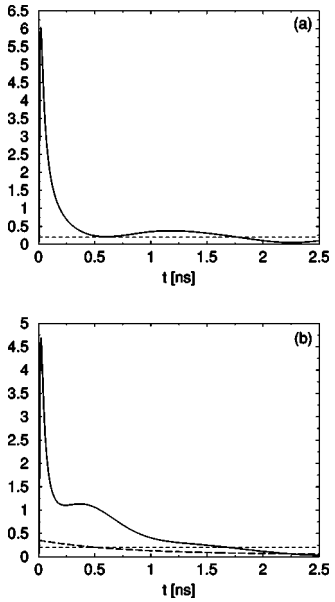

FIG. 3. The decay rate of population at $T=0$ in (a) and at $T=20$ mK in (b). The solid curve is our exact result, while the dashed lines are from using the Born-Markov apporoximation. $\Omega=1$ GHz, $\gamma=0.2$ GHz, and $\Lambda=100$ GHz.

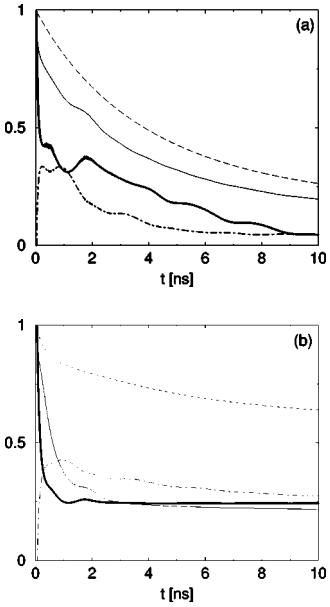

FIG. 4. The excited state populations and the leakage are plotted for super-Ohmic environment. $T=10$ mK in panel (a) and $T=50$ mK in panel (b). The thick (thin) solid curves is our exact result for super-Ohmic (Ohmic) case, while the dashed line is from using the Born-Markov apporoximation. $\Omega=1.5$ GHz, and $\Lambda=100$ GHz.

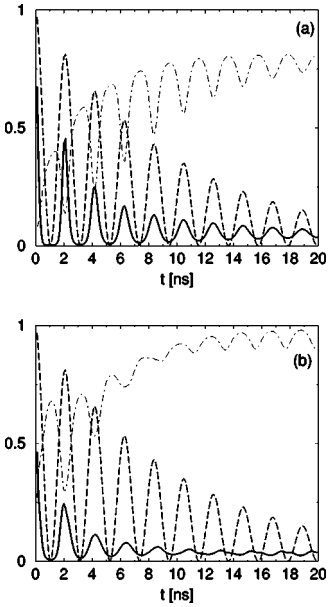

FIG. 5. Rabi oscillations and the leakage at $T=10$ mK are plotted for Ohmic environment in panel (a) and for super-Ohmic environment in panel (b). $E(t)=E_0\cos(\Omega t)$ with $E_0=2.0$. The thick solid curves are exact results, while the dashed curves are from using the Born-Markov approximation. $\Omega=1.5$ GHz, $\gamma=0.1$, and $\Lambda=100$ GHz.

Markovian approximation is constant for the two-level system (thin dashed line) but time-dependent for the multilevel system (thick dashed line). This is due to the fact that the Fock state is not an eigenstate of the interaction Hamiltonian (9). We will come back to this issue in the next section. The exact result exhibits a large initial growth similar to the $T=0$ case indicating that this comes from quantum fluctuations of the environment, then reaches asymptotically the value given by the Markovian multilevel case. In Fig. 4, the result for a super-Ohmic environment is plotted. Compared to the Ohmic case, the initial decay of the excited state population is much more drastic but it appears to saturate at late times. Thus if the initial decay is strong enough, the coherence in the system can be totally washed out at an early stage, a serious concern for the quantum devices. On the other hand, if it is small, the system can remain coherent for a long time. Note that our result disagrees markedly with the Markovian prediction over the entire time range.

In Fig. 5, the Rabi oscillations in the presence of an external sinusoidal pulse at the resonant frequency are plotted. The most notable difference between the exact results from the Markovian results is that the exact results show the low onset and low visibility for all times. The difference is more evident for the super-Ohmic case. Our figures also suggest that it is not easy to determine the characteristics of the environment only from the experimental Rabi oscillation data without the precise knowledge of the dissipation. The large increase of leakage is due to the resonant transition to higher level states. The leakage can be suppressed by detuning of the external field. Though increasing anharmonicity in the potential will also suppress these transitions to some extent, the initial rapid increase of leakage is unavoidable due to energy-time uncertainty relation. In the presence of tunneling with a biased potential, due to the dominance of resonant transitions to the continuum modes, we expect the result will be qualitatively similar to ours. In this case, the leakage in our model can be interpreted as the effect often attributed to tunneling. However, this rather corresponds to the hopping induced by environment to other metastable states. As the system-bath interaction increases, this hopping rate will increase similarly to the thermal hopping while the tunneling rate will be suppressed [22].

B. Discussion

Our nonperturbative calculation shows that at low enough temperatures, many conventional approaches based on the Born-Markov approximation can significantly underestimate the environment-induced decoherence beyond the weak system-bath coupling. In this regime, the visibility in Rabi oscillations in the exact calculation tends to be lower than what is expected in the Markovian approximation. Low visibility in Rabi oscillations is commonly observed in superconducting qubits [23–26]. The bath time scale is also important in causing the initial rapid decoherence and leakage; this is completely neglected in analysis based on the Born-Markov-RWA. This initial effect can manifest itself as an onset value of Rabi oscillations. In many practical implementations of qubits, the temperature of the environment compared to the bath cutoff frequency is small, $k_BT \ll \hbar\Lambda$, thus we are still in the low temperature regime.

For a sufficiently small quality factor Q, weak coupling approximation is no longer valid. Our results indicate that for Q smaller than $Q\sim 10-100$, there can be an extra suppres-

sion of Rabi oscillations such that their peaks largely deviate from the exponential curve. There is an enhancement of nonperturbative correction including the off-resonant contribution of the environment as temperature is lowered. For $Q > 1000$, nonperturbative effects are fairly suppressed. Nevertheless, they should appear as a *nonexponential* deviation from the exponential damping, depending on other parameters that can be extracted from the temporal evolution data.

The E2L-SBM approach gives a precise evaluation of the leakage due to the system's interaction with the environment and the external control field. For temperatures higher than the characteristic energy of the oscillator, the large leakage makes the qubit based on the choice of the lowest two levels ill-defined. During gate operations, this can become a serious problem and remedies for stabilizing the system such as using external pulse control may be necessary. Our result shows that the time scale associated with leakage is characterized by the dynamical time scale of both the system and the bath.

In realistic macro- or mesoscopic systems, the potential contains anharmonicity, which causes the deviation of the system dynamics from the harmonic motion. A measure of anharmonicity near the ground state can be given by the difference of energy level separation between the lowest levels $\omega_{01} \equiv \omega_1 - \omega_0$ and the excited levels $\omega_{12} \equiv \omega_2 - \omega_1$. When this difference is small, $\omega_{12} - \omega_{01} \ll \omega_{01}$, the initial short time evolution around a metastable state is well-described by the linear dynamics for any metastable state. When the correction to the energy level due to anharmonicity in the potential becomes important, it is necessary to include such an effect in our scheme. Although the large anharmonicity also prevents the leakage in the long term, the initial large leakage we saw cannot be completely eliminated as we mentioned before. When we apply our formalism to the metastable state, eventually the system state will leave the harmonic oscillator phase space into other metastable states via tunneling. The harmonic approximation of coherent dynamics is expected to be accurate at initial times when the time scales associated with these nonlinear effects are large compared to the decoherence time scale. In our example, the deviation from the Markovian prediction is evident in the very early stage of the system evolution up to $t \sim 1$ ns even for an intermediate temperature. For the realistic implementation of qubits, the underlying potential landscape leading to the discrete energy level is already known by design [23–26,30,31]. Our approach based on E2L-SBM is suitable in this situation and will give a more precise estimate of the open system dynamics than the one based on the conventional 2LS approximation. In particular, our results are directly relevent to the superconducting phase qubit models [23,24,31]. In the superconducting qubits, the major source of decoherence is the noise induced by the interaction with the current or charge sources mainly during the qubit manipulations. We have not considered other possible sources of decoherence such as the coupling to defects or nuclear and magnetic spins. Multilevel structure in the superconducting flux qubits was studied in [32] by Born-Markov approximation without control fields.

For many qubit models that involve electric charges, $1/f$ noise from background charge fluctuations are considered to be the dominant source of decoherence. Contrary to the $1/f$ noise, the effect of super-Ohmic environment is most evident in the ultrashort time range as shown in Fig. 4, which makes the detection of super-Ohmic environment a challenging task. Recent demonstration of spin-echo technique for the detection of $1/f$ noise [33] and the use of similar technique for the suppression of $1/f$ noise [34] are conducive to further clarifying decoherence in an super-Ohmic environment.

For the system-environment coupling we considered in Eq.(9), the Fock state is not an eigenstate of the interaction Hamiltonian and is subjected to a complex decay even under the Born-Markov approximation as shown in Sec. III C 2. Previous study in the high temperature limit indicates the pointer state which is stable under this system-environment coupling is a coherent state [7]. Our calculation based on the solutions of QBM indicates that, beyond the weak coupling regime, the environment-induced effect has a crucial impact on the system dynamics at an early stage. A pure and a mixed state initial conditions are studied in accord with the initialization scheme by cooling commonly used in quantum information processing [35]. Our results are robust under both initial conditions and also in accord with earlier studies of QBM including the preparation effect [4,36]. We expect that our results will hold for a more general class of initial conditions.

ACKNOWLEDGMENTS

This work was supported in part by ARDA Contract No. MDA90401/C0903. We thank colleagues in the Superconductivity Center at the University of Maryland, College Park, for showing us their phase-qubit experiments.

[1] *Decoherence and the Appearance of the Classical World in Quantum Theory*, edited by D. Giulini *et al.* (Springer, Berlin, 1996).

[2] J. P. Paz and W. H. Zurek, in *Coherent Matter Waves*, Les Houches Lectures Session LII (North-Holland, Amsterdam, 1999).

[3] W. G. Unruh, Phys. Rev. A **51**,992 (1995).

[4] U. Weiss, *Quantum Dissipative Systems* (World Scientific, Singapore, 1999).

[5] A. O. Caldeira and A. J. Leggett,Physica A **121**, 587 (1983); V. Hakim and V. Ambegaokar, Phys. Rev. A **32**, 423 (1985); F. Haake and R. Reibold, *ibid.* **32**, 2462 (1985); H. Grabert, P. Schramn, and G. L. Ingold, Phys. Rep. **168**, 115 (1988); W. G. Unruh and W. H. Zurek, Phys. Rev. D **40**, 1071 (1989); B. L. Hu and Y. Zhang, Mod. Phys. Lett. A **8**, 3575 (1993); Int. J. Mod. Phys. A **10**, 4537 (1995); J. J. Halliwell and A. Zoupas, Phys. Rev. D **52**, 7294 (1995); C. Anastopoulos and J. J. Halliwell, *ibid.* **51**, 6870 (1995).

[6] B. L. Hu, J. P. Paz, and Y. Zhang, Phys. Rev. D **45**, 2843 (1992).
[7] W. H. Zurek, S. Habib, and J. P. Paz, Phys. Rev. Lett. **70**, 1187 (1993).
[8] A. J. Leggett, S. Chakravarty, A. T. Dorsey, M. P. A. Fisher, A. Garg, and W. Zwerger, Rev. Mod. Phys. **59**, 1 (1987).
[9] L. Tian and S. Lloyd, Phys. Rev. A **62**, 050301 (2000).
[10] W. H. Luiselle, *Quantum Statistical Properties of Radiation* (Wiley, New York, 1990); D. Walls and G. J. Milburn, *Quantum Optics* (Springer, Berlin, 1995); H. J. Carmicheal, *Statistical Methods in Quantum Optics* (Springer, Berlin, 1999).
[11] J. P. Paz, S. Habib, and W. H. Zurek, Phys. Rev. D **47**, 488 (1993).
[12] K. Shiokawa and R. Kapral, J. Chem. Phys. **117**, 7852 (2002).
[13] R. P. Feynman and F. L. Vernon, Ann. Phys. (N.Y.) **24**, 118 (1963).
[14] E. Wigner, Phys. Rev. **40**, 749 (1932).
[15] L. Mandel and E. Wolf, *Optical Coherence and Quantum Optics* (Cambridge University Press, Cambridge, England, 1995).
[16] J. Twamley, Phys. Rev. D **48**, 5730 (1993).
[17] G. M. Palma, K.-A. Suominen, and A. K. Ekert, Proc. R. Soc. London, Ser. A **452**, 567 (1996).
[18] C. Cohen-Tannoudiji, J. Dupont-Roc, and G. Grynberg, *Atom-Photon Interactions* (Wiley, New York, 1992).
[19] G. W. Ford and R. F. O'Connell, Physica A **243**, 377 (1997).
[20] D. Ahn, J. Lee, M. S. Kim, and S. W. Hwang, Phys. Rev. A **66**, 012302 (2002).
[21] D. Loss and D. P. DiVincenzo, e-print cond-mat/0304118.
[22] A. O. Caldeira and A. J. Leggett, Ann. Phys. (N.Y.) **149**, 374 (1983).
[23] Y. Yu, S. Han, X. Chu, S. I. Chu, and Z. Wang, Science **296**, 8898 (2002).
[24] J. M. Martines, S. Nam, J. Aumentado, and C. Urbina, Phys. Rev. Lett. **89**, 117901 (2002).
[25] D. Vion, A. Aassime, A. Cottet, P. Joyez, H. Pothier, C. Urbina, D. Esteve, and M. H. Devoret, Science **296**, 886 (2002).
[26] I. Chiorescu, Y. Nakamura, C. H. P. M. Harmans, and J. E. Mooij, Science **299**, 1869 (2003).
[27] A. Garg and G. H. Kim, Phys. Rev. Lett. **63**, 2512 (1989); P. M. V. B. Barone and A. O. Caldeira, Phys. Rev. A **43**, 57 (1991); S. A. Egorov and B. J. Berne, J. Chem. Phys. **107**, 6050 (1997).
[28] P. Pechukas, in *Large-Scale Molecular Systems*, Vol. 258 of *NATO Advanced Study Institute*, edited by W. Gaus *et al.* (Plenum, New York, 1991).
[29] M. Tokuyama and H. Mori, Prog. Theor. Phys. **55**, 411 (1975); N. Hashitsume, F. Shibata, and M. Shingu, J. Stat. Phys. **17**, 155 (1977).
[30] Y. Makhlin, G. Schön, and A. Shnirman, Rev. Mod. Phys. **73**, 357 (2001).
[31] A. J. Berkley, H. Xu, R. C. Ramos, M. A. Gubrud, F. W. Strauch, P. R. Johnson, J. R. Anderson, A. J. Dragt, C. J. Lobb, and F. C. Wellstood, Science **300**, 1548 (2003).
[32] G. Burkard, R. H. Koch, and D. P. DiVincenzo, Phys. Rev. B **69**, 064503 (2004).
[33] Y. Nakamura, Yu. A. Pashkin, T. Yamamoto, and J. S. Tsai, Phys. Rev. Lett. **88**, 047901 (2002).
[34] K. Shiokawa and D. A. Lidar, Phys. Rev. A **69**, 030302 (2004); H. Gutmann, F. K. Wilhelm, W. M. Kaminsky, and S. Lloyd, e-print cond-mat/0308107; L. Faoro and L. Viola, e-print quant-ph/0312159; G. Falci, A. D'Arrigo, A. Mastellone, and E. Paladino, e-print cond-mat/0312442.
[35] M. A. Nielsen and I. L. Chuang, *Quantum Computation and Quantum Information* (Cambridge University Press, Cambridge, England, 2000).
[36] L. D. Romero, and J. P. Paz, Phys. Rev. A **55**, 4070 (1997).